2014 IEEE International Conference on Robotics & Automation (ICRA)
Hong Kong Convention and Exhibition Center
May 31 - June 7, 2014. Hong Kong, China

Design of a New Counter-Balancing Stackable Mechanism

Jong-Tae Seo, Jae Hong Woo, Hoon Lim, and Byung-Ju Yi, *Member, IEEE*

***Abstract*— This paper describes design and application of a novel counter-balancing stackable parallel mechanism. The stackable mechanism is designed by combining a five-bar and a couple of parallelograms. This design allows a compact design and wide workspace as compared to prior parallel type counter-balancing mechanisms. A linear geometry of this mechanism guarantees static balancing in the whole workspace. This mechanism was successfully applied to otologic.**

I. Introduction

Counter-balancing mechanism has been widely employed to compensate for gravity load of links and resultantly increase the payload of the robot. Extensive applications can be found in automotive industry, industrial robot, service robot, home furniture, medical devices, construction, and so on.

In the design of haptic mechanism, Lessard, et al [1] designed a 5-bar gravity-balancing parallel mechanism by using torsion springs at joints. Tahmasebi, et al [2] designed a 5-bar parallel mechanism by using actuator as a counter-weight. Wang and Gosselin [3-4] designed 3-DOF and 6-DOF spatial parallel mechanisms by attaching a counter-weight and spring at some links and joints. Laliberte and Gosselin [5] investigated counter-balancing of a 3-DOF planar parallel mechanism in a similar manner. In the design of service robot, Park, et al. [6] designed a counter-balancing serial mechanism by attaching a spring at each joint. Herder [7] presented a design method for statically balanced spring mechanisms.

Specifically, need for counter-balancing mechanism grows much in the area of medical devices. The medical microscope being used in operation room is such an example. Nakamura, et al [8-9] designed a gravity-balancing parallelogram mechanism by using an adjustable moment arm. Nakamura, et al [10] designed a gravity-balancing serial mechanism using timing belt by attaching a counter-weight at the end point of the lower link. Nakamura [11] designed a balancing chair for medical apparatus. In the design of rehabilitation devices, Agrawal and Agrawal [12] designed a gravity-balancing auxiliary parallelogram mechanism by using springs at some links and joints. However, most of previous works have not paid much attention to the open-loop stability under static equilibrium. Seo, et al [13] initially analyzed the open-loop stability of a counter-balancing parallel mechanism. A general stiffness model was employed as a measure for open-loop stability. The zero stiffness is found an ideal case implying static equilibrium at all workspace.

As an extension of Seo, et al [13], this paper aims at developing a novel counter-balancing mechanism, which has a larger workspace and ideal open-loop stability in terms of stiffness by employing stackable design architecture of kinematic linkages. Lee, et al [14] initially proposed such stackable design architecture in the design of slim end-effector for single port access surgery. However, the gravity load of the mechanism was not taken into account because of its small size and the whole structure was constructed only by stacking a couple of four-bar mechanisms. This paper proposes another type of stackable mechanism by combining a five-bar and a couple of parallelograms. This design allows a compact design as compared to the four-bar based design and provides a linear geometry which yields zero stiffness in the whole workspace (i.e., an ideal open-loop stability).

The procedure of this paper is as follows. In section II, a new stackable mechanism is introduced. The kinematic and static models are derived in section III. In section IV, we propose a special design of the stackable mechanism for the otologic surgery. Workspace analysis and kinematic optimization are performed. A prototype was developed and tested using a phantom based on a patient's data of temporal bone. Finally, we draw conclusion in section V.

II. Design of Counter-Balancing

A. Stackable Parallel Mechanism

Fig. 1 shows a stackable parallel mechanism. This mechanism is constructed by stacking one double parallelogram over one five-bar. This process can be continued by stacking a triple parallelogram over it. So, this stackable mechanism architecture has 'Self-Similarity' and 'Recursiveness' characteristics. Thus, it can be extended to N-DOF mechanism in general.

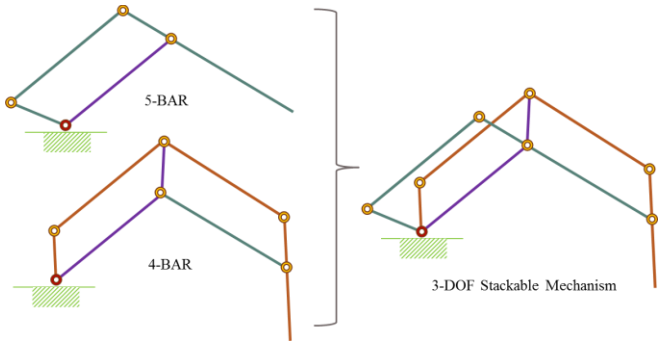

Figure 1. How to construct a stackable mechanism.

J. -T. Seo is with the Department of Mechatronics Engineering, Hanyang University, Ansan, Korea (e-mail: jt1000je@nate.com).

J. H. Woo is with the Department of Intelligent Robot Engineering, Hanyang University, Ansan, Korea (e-mail: jokers12@nate.com).

H. Lim is with the Department of Electronic, Electrical, Control and Instrumentation Engineering, Hanyang University, Ansan, Korea (e-mail: jokers12@ nate.com and hoonlim78@gmail.com).

B. -J. Yi is with the Department of Electronic Systems Engineering, Hanyang University, Ansan, Korea (corresponding author to provide phone: +82-31-400-5026; fax: +82-31-400-5027; e-mail: bj@ hanyang.ac.kr).

B. Counter-Balancing

Fig. 2 shows a 3-DOF (degree of freedom) stackable mechanism with counter-weights. Counter-balancing method is based on the joint space where counter-weights (M_1, M_2, M_3, M_4, M_5) can be hanged at some of the extended ends of proximal links (J_1, J_2, J_3, J_4, J_5) as shown in Fig. 2. It is noted that only three counter-weights and three extended link lengths can be chosen among 5 candidates, respectively, since the mechanism has 3-DOF. This choice depends on several design constraints of this mechanism.

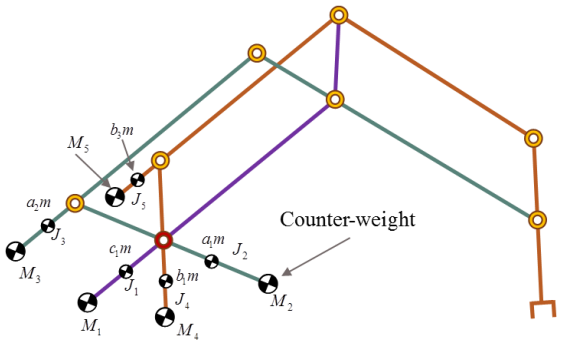

Figure 2. Counter-balancing mechanism.

III. Kinematics and Dynamics

A. Mobility analysis

Fig. 3 denotes the Fractal model for mobility analysis. The mobility can be confirmed from the Grubler's mobility formula as having 3-DOF from

$$M = D(L-1) - \sum_{i=1}^{J}(D-F_i) = 3(10-1) - 12(3-1) = 3,$$

where D is the maximum motion degree of link (3 in plane), L is the number of links including the ground (10), J is the number of joints (12), and F_i is the motion degree of the i^{th} joint (1).

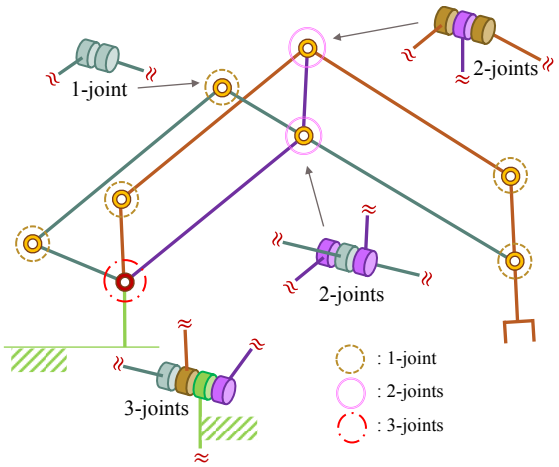

Figure 3. Mobility analysis

B. Forward Kinematics

Fig. 3 denotes the kinematic model of the stackable mechanism. Since the mechanism has 3-DOF, we can define three independent joints. Three proximal joints (θ_1, θ_3, θ_6) are decided as the independent joints and it is named as $\underline{\phi}_a$. The rest joints are set as the dependent joints (θ_2, θ_4, θ_5, θ_7, θ_8, θ_9) and it is named as $\underline{\phi}_p$.

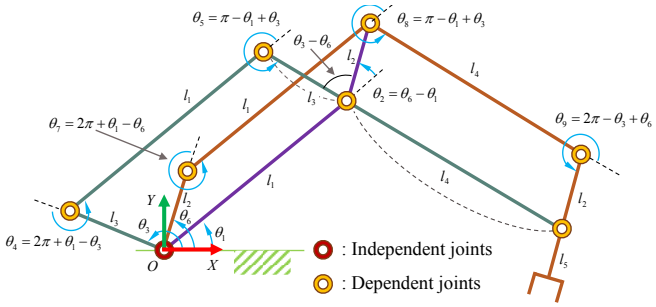

Figure 4. Kinematic model.

Forward kinematics can be denoted simply as shown in Eq. (1) because constrained conditions of the dependent joints are known (see Fig. 4).

$$\begin{bmatrix} x \\ y \\ \Phi \end{bmatrix} = \begin{bmatrix} l_1\cos\theta_1 - l_4\cos\theta_3 - l_5\cos\theta_6 \\ l_1\sin\theta_1 - l_4\sin\theta_3 - l_5\sin\theta_6 \\ \pi + \theta_6 \end{bmatrix}. \quad (1)$$

And analyzing the closed-chain geometry given in Fig. 4, the relationship between the operational output and the independent joins can be obtained by partial differential of the Eq. (1) with respect to time as follows

$$\dot{\underline{u}} = \left[G_a^u\right]\dot{\underline{\phi}}_a, \quad (2)$$

where

$$\left[G_a^u\right] = \begin{bmatrix} -l_1\sin\theta_1 & l_4\sin\theta_3 & l_5\sin\theta \\ l_1\cos\theta_1 & -l_4\cos\theta_3 & -l_5\cos\theta_6 \\ 0 & 0 & 1 \end{bmatrix}. \quad (3)$$

Noting that all the dependent joint angles can be expressed in terms of independent joint angles in Fig. 4, the relationship between the dependent joints and the independent joints can be directly obtained as follows

$$\dot{\underline{\phi}}_p = \left[G_a^p\right]\dot{\underline{\phi}}_a, \quad (4)$$

where

$$\left[G_a^p\right] = \begin{bmatrix} -1 & 0 & 1 \\ 1 & -1 & 0 \\ -1 & 1 & 0 \\ 1 & 0 & -1 \\ -1 & 1 & 0 \\ 0 & -1 & 1 \end{bmatrix}. \quad (5)$$

Using the virtual work principle, the torque $\underline{\tau}_p$ of the dependent joints can be expressed as an effective torque $\underline{\tau}_a^{'}$ at the independent joints as follows

$$\underline{\tau}_a^{'} = \left[G_a^p \right]^T \underline{\tau}_p, \tag{6}$$

where $\underline{\tau}_p = (\tau_2 \ \tau_4 \ \tau_5 \ \tau_7 \ \tau_8 \ \tau_9)^T$.

C. Statics

A mechanism is said statically-balanced if the weight of links does not require any torque (or force) at the actuators under static conditions, for any configuration of the mechanism. A mechanism with constant potential energy for any possible configuration is also statically-balanced. Two approaches, namely counterweights and elastic elements (springs), can be used to obtain statically balanced mechanisms [16]. Counterweights adjust the center of mass of the mechanism to be constant in the direction of the gravity vector. In other words, counterweights adjust the gravitational potential energy of this system to be constant.

For static balancing of the stackable mechanism, an effective torque to compensate for the gravity loads of the stackable mechanism should be derived. For this, we consider an open-chain model as Fig. 4 by cutting joints. Then, we obtain the effective torque for each open-chain and using the virtual work principle, we transfer the effective torques at all Lagrangian coordinates (all joints) to that at independent coordinates (active inputs).

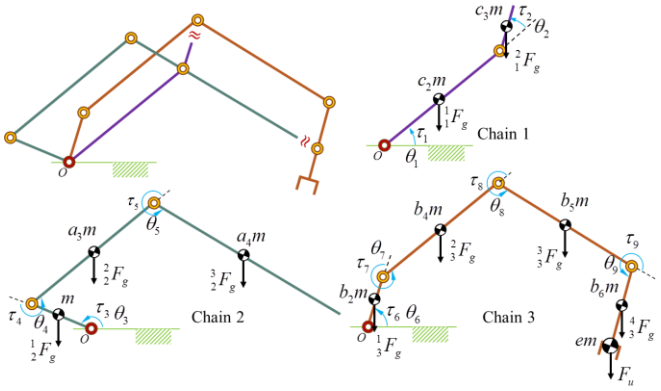

Figure 5. Open-chain model

For the first open-chain, the required torque of each joint for static balancing of the mechanism is derived as

$$\begin{aligned}\tau_1 = &-\frac{l_1}{2} c_2 mg \cos\theta_1 - \left\{ l_1 \cos\theta_1 + \frac{l_2}{2} \cos(\theta_1 + \theta_2) \right\} c_3 mg \\ &+ \frac{J_1}{2} c_1 mg \cos\theta_1 + J_1 M_1 g \cos\theta_1\end{aligned} \tag{7}$$

$$\tau_2 = -\frac{l_2}{2} c_3 mg \cos(\theta_1 + \theta_2), \tag{8}$$

where m denotes the mass of the proximal link of the open-chain 2, and the mass of other links will be expressed as qm, where q is an arbitrary, positive real number. Applying the dual relationship between the independent joint set and the dependent joint set to Eq. (7) and (8), the required joint torque can be expressed as those at independent joints.

$$\begin{aligned}\tau_1 = &\left\{ J_1 \left(\frac{c_1 m}{2} + M_1 \right) - l_1 m \left(\frac{c_2}{2} + c_3 \right) \right\} g \cos\theta_1 \\ &- \frac{l_2}{2} c_3 mg \cos\theta_6\end{aligned} \tag{9}$$

$$\tau_2 = -\frac{l_2}{2} c_3 mg \cos\theta_6. \tag{10}$$

Similarly to the first open-chain, the required joint torques for the second chain are

$$\begin{aligned}\tau_3 = &\left\{ \frac{J_2}{2} a_1 m - \frac{l_3}{2} m + J_2 M_2 - l_3 a_3 m - l_3 a_2 m - l_3 M_3 \right. \\ &\left. - \left(l_3 - \frac{l_3 + l_4}{2} \right) a_4 m \right\} g \cos\theta_3 \\ &- \left(\frac{l_1}{2} a_3 m - \frac{J_3}{2} a_2 m - J_3 M_3 + l_1 a_4 m \right) g \cos\theta_1\end{aligned} \tag{11}$$

$$\begin{aligned}\tau_4 = &\left(\frac{J_3}{2} a_2 m - \frac{l_1}{2} a_3 m + J_3 M_3 - l_1 a_4 m \right) g \cos\theta_1 \\ &+ \frac{l_3 + l_4}{2} a_4 mg \cos\theta_3\end{aligned} \tag{12}$$

$$\tau_5 = \frac{(l_3 + l_4)}{2} a_4 mg \cos\theta_3. \tag{13}$$

Similarly to the first open-chain, the required joint torques for the third chain are

$$\begin{aligned}\tau_6 = &\left\{ \left(\left(l_2 + \frac{l_5}{2} \right) b_7 - \frac{l_2}{2} b_2 - l_2 b_3 - l_2 b_4 - l_2 b_5 - \frac{l_2}{2} b_6 - l_2 e \right. \right. \\ &\left. + (l_2 + l_5) e \right) m + \frac{J_4}{2} b_1 m + J_4 M_4 - l_2 M_5 \Big\} g \cos\theta_6 \\ &- \left\{ l_1 \left(\frac{1}{2} b_4 + b_5 + b_6 + e \right) m - \frac{J_5}{2} (b_3 m - 2M_5) \right\} g \cos\theta_1 \\ &+ \left\{ \frac{l_3 + l_4 - l_2}{2} b_5 + l_4 b_6 + l_4 e \right\} mg \cos\theta_3.\end{aligned} \tag{14}$$

$$\begin{aligned}\tau_7 = &\left(\frac{l_2}{2} b_6 + \left(l_2 + \frac{l_5}{2} \right) b_7 + (l_2 + l_5) e \right) mg \cos\theta_6 \\ &- \left\{ l_1 \left(\frac{1}{2} b_4 + b_5 + b_6 + e \right) m - \frac{J_5}{2} (b_3 m - 2M_5) \right\} g \cos\theta_1 \\ &+ \left\{ \frac{l_3 + l_4 - l_2}{2} b_5 + l_4 b_6 + l_4 e \right\} mg \cos\theta_3\end{aligned} \tag{15}$$

$$\begin{aligned}\tau_8 = &\left\{ \frac{l_2}{2} b_6 + \left(l_2 + \frac{l_5}{2} \right) b_7 + (l_2 + l_5) e \right\} mg \cos\theta_6 \\ &+ \left\{ \frac{l_3 + l_4 - l_2}{2} b_5 + l_4 (b_6 + e) \right\} mg \cos\theta_3\end{aligned} \tag{16}$$

$$\tau_9 = \left\{\frac{l_2}{2}b_6 + \left(l_2 + \frac{l_5}{2}\right)b_7 + (l_2 + l_5)e\right\} mg\cos\theta_6. \quad (17)$$

Now, the total torque transferred to the independent joints is expressed and simplified as

$$\begin{aligned}\underline{\tau}_a^* &= \underline{\tau}_a + \underline{\tau}_a' \\ &= \begin{bmatrix} k_1 & \underline{0} & \\ & k_2 & \\ \underline{0} & & k_3 \end{bmatrix} \begin{bmatrix} \cos\theta_1 \\ \cos\theta_3 \\ \cos\theta_6 \end{bmatrix},\end{aligned} \quad (18)$$

where $\underline{\tau}_a = (\tau_1\ \tau_3\ \tau_6)^T$ and

$$\begin{aligned} k_1 &= \left\{-\frac{l_1}{2}m(a_3 + 2a_4 + b_4 + 2b_5 + 2b_6 + c_2 + 2c_3 + e)\right. \\ &\quad \left. + \frac{J_3}{2}(a_2 m + 2M_3)\right\} g \\ k_2 &= \left\{l_4(b_6 + e)m - \frac{l_3}{2}(1 + 2a_2 + 2a_3)m - \left(l_3 - \frac{l_3 + l_4}{2}\right)a_4 m\right. \\ &\quad \left. + \frac{1}{2}(l_3 + l_4 - l_2)b_5 m + \frac{J_2}{2}(2M_2 - a_1 m) - l_3 M_3\right\} g \\ k_3 &= \left\{-\frac{l_2}{2}(b_2 + 2b_4 + 2b_5 + 2b_6 + c_3 + 2e)m\right. \\ &\quad \left. + \frac{(l_2 + l_5)}{2}em + \frac{J_4}{2}(2M_4 + b_1 m)\right\} g. \end{aligned} \quad (19)$$

It is noted from Eq. (18) and (19) that all coefficients k_i ($i = 1 \sim 3$) is constant. It is also noted that the static balancing condition of the stackable mechanism has nothing to do with the joint angles of the three independent coordinates, because we just need to manipulate three equations $k_1 = k_2 = k_3 = 0$ for static equilibrium. As a result, the counter-weights and extended link lengths can be sought.

D. General Stiffness Modeling

In a state of static equilibrium among actuator torques, gravity loads at links, and externally applied loads, the system tends to oscillate like a spring once the system is perturbed from its equilibrium state. Yi and Freeman [16] introduced a general stiffness model for general closed-chain mechanism driven by abundant number of actuators. Seo, et al [13] modified the general stiffness model by including the effect of counter-weight and employed the stiffness model to analyze the open-loop stability of the system. It was concluded that if the counter-balanced system yields a null stiffness matrix, the system results in zero resorting force upon perturbation. This feature is important in the design of passive hands-on devices, because the surgeon is able to control the mechanism freely in the 3-dimensional space without feeling any gravity load of the system.

For the stackable mechanism, the stiffness model will be analyzed. In a state of static balancing, the effective torque with respect to the independent joints is zero (i.e., $\underline{\tau}_a^* = 0$). Differentiating τ_a^* with respect to the independent joints, the stiffness model is obtained as

$$\left[K_{aa}^*\right] = -\frac{\partial \underline{\tau}_a^*}{\partial \underline{\phi}_a}. \quad (20)$$

Substituting Eq. (17) into Eq. (18), we have

$$\left[K_{aa}^*\right] = -\frac{\partial [C]}{\partial \underline{\phi}_a} \cdot \begin{bmatrix} \cos\theta_1 \\ \cos\theta_3 \\ \cos\theta_6 \end{bmatrix} - [C] \cdot \frac{\partial}{\partial \underline{\phi}_a} \begin{bmatrix} \cos\theta_1 \\ \cos\theta_3 \\ \cos\theta_6 \end{bmatrix}, \quad (21)$$

where

$$[C] = \begin{bmatrix} k_1 & 0 & 0 \\ 0 & k_2 & 0 \\ 0 & 0 & k_3 \end{bmatrix}. \quad (22)$$

It is noted that the first term of Eq. (21) is zero because the matrix $[C]$ is always constant. The second term is also zero because $[C]$ denotes counter-balancing condition of the mechanism and thus it is a null matrix. As a result, the stiffness matrix with respect to the independent joints is a null matrix. Physically speaking, the stackable mechanism not only maintains a static equilibrium at all workspace of this mechanism but also does not produce any restoring force upon any initial displacement (or perturbation). This is due to linear geometry of the stackable mechanism as noted in Eq. (18). Thus, we can interpret the static balancing problem as design of linear geometry problem.

Using three equation given by $k_1 = k_2 = k_3 = 0$, three counter-weights and corresponding moment arms can be obtained. In this case, the other two counter-weights (i.e., (M_1, M_5) are set as zero values.

IV. Application

A. Target application

The stackable mechanism introduced in this paper has many potential applications. We employ this mechanism as a positioner for precise otologic surgery. Fixing the angle θ_6 as $3\pi/2$ and adding one rotational joint θ_0 along the y-axis as shown in Fig. 7, the stackable mechanism produces translational 3-DOF motion while preserving the counter-balancing characteristic.

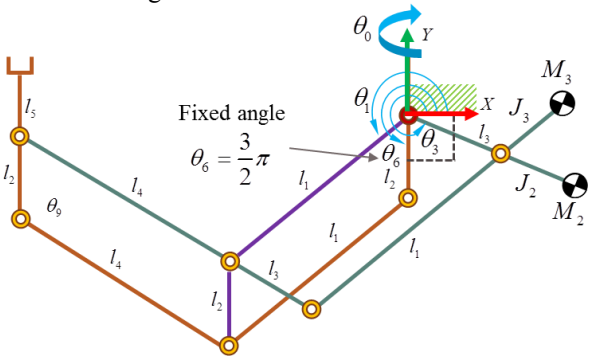

Figure 6. Translational 3-DOF model.

At the distal end of the translational 3-DOF stackable mechanism, we can mount any end-effector for special

purpose. In the otologic surgery, we employ a drill as a tool to remove bones to reach to the target lesion inside the temporal bone. A rotational 3DOF was designed and mounted at the end of the translational mechanism to control orientation of the drill tool. Including the mass of the rotational device, the counter-weights and the extended link lengths can be decided. In this case, only two constraint equations ($k_1 = k_2 = 0$) are taken into account for static balancing.

Table I includes kinematic and dynamic parameters for simulation. The kinematic and dynamic parameters associated with the counter-weighting design are initially set as $(M_2 = 0.2,\ M_3 = 1.5kg,\ J_2 = -250mm,\ J_3 = 162.3mm)$, though optimal parameters can be also sought for a specific task description. The static balancing behavior of the stackable mechanism is verified using a commercially-available software called 'DAFUL' made of virtual motion Co [17]. It is shown from Fig. 6 that at all workspace the stackable mechanism sustains static equilibrium.

TABLE I. KINEMATIC PARAMETERS

Link Parameters	Dynamic Parameters
$l_1 = l_4 = 200\,mm$	Mass of the each link-weight at the first chain
$l_2 = l_3 = 100\,mm$	$c_1m = 0.000\,kg$
$l_5 = 0\,mm$	$c_2m = 0.065\,kg$
$J_1 = 0\,mm$	$c_3m = 0.040\,kg$
$J_2 = 150\,mm$	Mass of the each link-weight at the second chain
$J_3 = 150\,mm$	$m = 0.050\,kg$
$J_4 = 0\,mm$	$a_2m = 0.000\,kg$
$J_5 = 0\,mm$	$a_3m = 0.065\,kg$
	$a_4m = 0.085\,kg$
	Mass of the each link-weight at the third chain
	$b_1m = 0.000\,kg$
	$b_2m = 0.000\,kg$
	$b_4m = 0.060\,kg$
	$b_5m = 0.060\,kg$
	$b_6m = 0.060\,kg$
	$em = 0.877\,kg$
	Mass of the lower counter-weight
	$M_2 = 0.106\,kg$
	$M_3 = 1.623\,kg$

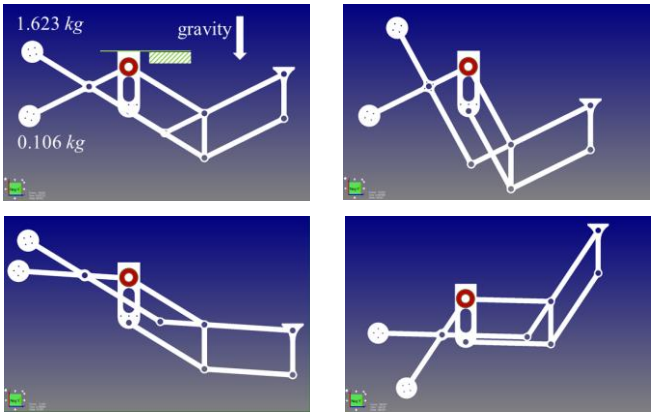

Figure 7. Simulation results of the counter-balancing.

The attached video clip 1 demonstrates the motion of the counter-balancing characteristic of this resulting 6-DOF device.

B. Implementation

Human-robot collaboration approach has been popular for precise control. Steady-hand approach is a typical method to reflect the surgeon's intention with assistance of robot [18]. However, the approach using such admittance-type robots driven by high-geared motor used for speed reduction and force amplification is too sluggish, compared to the operational speed of the drilled task performed by surgeon. For operation at high speed, gravity compensation and dynamic inertial load should be compensated in the robot design. Rather than using active type robots, we employ the proposed stackable mechanism, which is a passive type device but designed to satisfy operational requirements in otologic surgery by implementing static-balancing design and minimization of the total mass of the system.

The developed stackable mechanism is applied to mastoidectomy which is a surgical procedure that removes an infected portion of the mastoid bone. The roles of the robot in this task are defined as (i) tool holder, (ii) navigation sensor, (iii) brake.

Otologic surgery requires high accuracy, because there are many important arteries and nerves located closely to the target. Thus, only a skillful doctor is allowed to perform the otologic surgery, since it is a very difficult surgery. Furthermore, a resident should have many experiences in order to make himself or herself familiar with the skill in the otologic surgery. However, chance of surgery is limited to novice surgeons. Thus, a surgical robotic system is required to help young surgeon train minimally invasive surgery while preserving safety in surgery.

Navigation system is one of important components of the robotic system. Some of important organs inside the temporal bone (such as facial nerves and carotid artery) are invisible during surgery, because these parts are located under the mastoid bone. Thus, image-guided navigation and warning system help surgeon avoid damaging important organs inside the temporal bone. We developed forbidden-region virtual fixtures to prevent the drill bit from entering into forbidden regions of the workspace. For this, we develop a 3D facial nerve model based on the CT data of a patient and the forbidden-region containing the facial nerve and a margin of 3 mm.

Using the 3D model of the temporal bone based on a patient's CT image, a human-robot collaboration control is performed and evaluated. Through the registration of the robot coordinate into the image coordinate, the surgeon was able to check if the drilling does not damage the important organs inside the temporal bone. Furthermore, using the warning algorithm, a safety problem could also be handled.

Figure 8 is the system configuration of the otologic surgical robot system. The system consists of a surgical robot, an image-guided navigation software, and an optical tracker. In order to integrate the navigation system and the robotic system, a patient coordinate to CT-image coordinate registration is required.

The surgeon can monitor a target lesion, relevant organs, and the surgical drill in real-time by the image-guided navigation system. Fig. 9 is a navigation software including the warning algorithm. The warning algorithm helps the surgeon prevent the surgical drill burr from entering into critical organs. If the drill burr reaches to the critical organ, the warning algorithm is activated by flickering the navigation view with a warning sound. And the robot automatically stops by applying the magnetic brake installed at joints of the mechanism.

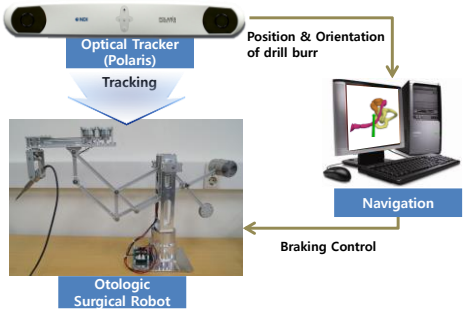

Figure 8. System configuration.

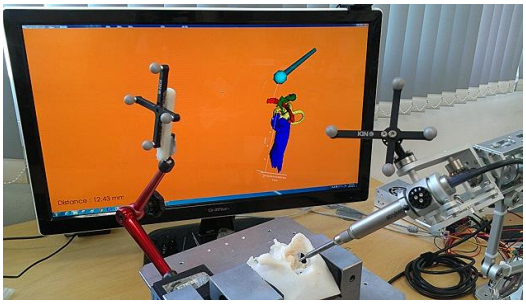

Figure 9. Navigation software including warning algorithm.

The static balancing of the mechanism helps the surgeon manipulate the tool attached to the distal end freely without feeling much resisting force. The attached video clip 2 demonstrates that using the 6-DOF (3-DOF translational motion and 3-DOF rotational motion) device, the user was able to perform the mastoidectomy successfully with the aid of the navigation software.

V. Conclusions

Contribution of this paper is proposition of a new stackable mechanism which can be extended to N-DOF in general. The linear geometry of the stackable mechanism helps designing a counter-balanced mechanism. Through application to otologic surgery, usefulness of the stackable mechanism has been proven. Future work involves general applications of this counter-balancing mechanism and task-specific optimization.

Acknowledgment

This work was supported by the BK21 Plus Program (Future-oriented innovative brain raising type, 22A20130012806) funded by the Ministry of Education (MOE, Korea) and National Research Foundation of Korea (NRF), supported by the Technology Innovation Program (10040097) funded by the Ministry of Trade, Industry and Energy Republic of Korea (MOTIE, Korea), supported by GRRC program of Gyeonggi Province (GRRC HANYANG 2013-A02), and financially supported by the Ministry of Trade, Industry and Energy (MOTIE) and Korea Institute for Advancement in Technology (KIAT) through the Workforce Development Program in Strategic Technology, supported by the MOTIE(The Ministry of Trade, Industry and Energy), Korea, under the Robotics-Specialized Education Consortium for Graduates support program supervised by the NIPA(National IT Industry Promotion Agency) (H1502-13-1001).

References

[1] S. Lessard, P. Bigras, and I. A. Bonev, "A new medical parallel robot and its static balancing optimization," *ASME Trans. J. Med. Devices*, vol. 1, no. 4, 2007, pp. 272-278.

[2] A.M. Tahmasebi, B. Taati, F. Mobasser, and K. Hashtrudi-Zaad, "Dynamic parameter identification and analysis of a PHANToM™ haptic device," in *Proc. of IEEE Conf. on Control Applications*, pp. 1251-1256, 2005.

[3] J. Wang and C.M. Gosselin, "Static balancing of spatial three-degree-of –freedom parallel mechanisms," *Mechanism and Machine Theory*, vol. 34, 1999, pp. 437-452.

[4] C.M. Gosselin and J. Wang, "Static balancing of spatial six-degree-of-freedom parallel mechanisms with revolute actuators," *Journal of Robotic Systems*, vol. 17, no. 3, 2000, pp. 159-170.

[5] T. Laliberte, C.M. Gosselin, and M. Jeam, "Static balancing of 3-DOF planar parallel mechanisms," *IEEE/ASME Trans. on Mechatronics*, vol. 4, no. 4, 1999, pp. 363-377.

[6] J.-J. Park, Y.-J. Lee, J.-B. Song, and H.-S Kim, "Safe joint mechanism based on nonlinear stiffness for safe human-robot collision," in *Proc. of IEEE Int. Conf. on Robotics and Automation*, pp. 2177-2182, 2008.

[7] J. Herder, "Energy-free systems : theory, conception, and design of statically balanced spring mechanism," Ph.D. dissertation, Delft University of Technology, Denmark, 2001.

[8] K. Nakamura, M. Dol, T. Hashimoto, and M. Nakamura, "Holding arm apparatus for medical tool," U.S. Patent 0162476 A1, 2011.

[9] K. Nakamura, "Biaxial balance adjusting structure for medical stand apparatus," U.S. Patent 5 480 114, 1996.

[10] K. Nakamura, M. Dol, and M. Nakamura, "Medical stand apparatus," U.S. Patent 6 045 104, 2000.

[11] K. Nakamura and T. Ota, "Balancing char," U.S. Patent 5 927 815, 1999.

[12] A. Agrawal and S.K. Agrawal, "Design of gravity balancing leg Orthosis using non-zero free length springs," *Mechanism and Machine Theory*, vol. 40. 6, 2005, pp. 693-709.

[13] J.-T. Seo, J.H. Woo, H. Lim, J. Chung, W. K. Kim, and B.-J. Yi, "Design of an antagonistically counter-balancing parallel mechanism," in *Proc. of IEEE/RSJ Int. Conf. on Intelligent Robots and Systems*, 2013.

[14] H. Lee, Y. Choi, and B.-J. Yi, "Stackable 4-BAR manipulators for single port access surgery," *IEEE/ASME Trans. Mechatronics*, vol. 17, no. 1, 2012, pp. 157-166.

[15] I. Ebert-Uphoff, C. M. Gosselin, and T. Laliberté, "Static balancing of spatial parallel platform mechanisms—revisited," Journal of Mechanical Design, vol. 122, 2000, p. 43.

[16] B.–J. Yi, and R.A. Freeman, "Geometric analysis of antagonistic stiffness in redundantly actuated parallel mechanisms," *Journal of Robotic Systems*, vol. 10, no. 5, 1993, pp. 581-603.

[17] www.virtualmotion.co.kr

[18] J. Hong, H. Lim, B.-J. Yi, S. H. Lee, J. H. Jeong, N. Matsumoto, M. Oka, S. Komune, and M. Hashizume, "Phantom experiment of an ear surgery robot for automatic mastoidectomy," in *Proc. of Int. Conf. on the Advanced Mechatronics*, pp. 295-300, 2010.